ARTICLES

Analytical model of non-uniform charge distribution within the gated region of GaN HEMTs

Amgad A. Al-Saman[1, 2], Eugeny A. Ryndin[3], Xinchuan Zhang[2], Yi Pei[2, †], and Fujiang Lin[1, †]

[1]School of Microelectronics, University of Science and Technology of China, Hefei 230026, China

[2]Dynax Semiconductor Inc., Suzhou 215300, China

[3]Department of Micro- and Nanoelectronics, Saint Petersburg Electrotechnical University, Saint Petersburg 197376, Russia

Abstract: A physics-based analytical expression that predicts the charge, electrical field and potential distributions along the gated region of the GaN HEMT channel has been developed. Unlike the gradual channel approximation (GCA), the proposed model considers the non-uniform variation of the concentration under the gated region as a function of terminal applied voltages. In addition, the model can capture the influence of mobility and channel temperature on the charge distribution trend. The comparison with the hydrodynamic (HD) numerical simulation showed a high agreement of the proposed model with numerical data for different bias conditions considering the self-heating and quantization of the electron concentration. The analytical nature of the model allows us to reduce the computational and time cost of the simulation. Also, it can be used as a core expression to develop a complete physics-based transistor $\mathrm{I}\mathrm{V}$ model without GCA limitation.

Key words: AlGaN/GaN (HEMTs); 2DEG; charge distribution; electron mobility; hydrodynamic model; channel temperature

1. Introduction

The high piezoelectrical effect and controllable mismatch in AlGaN/GaN HEMT transistor allow us to achieve a high value of sheet concentration and, consequently, high delivered output power[1−5]. The power and frequency performance of GaN HEMTs widen their application in high-speed R.F. integrated circuits[2, 3]. Modeling of the 2DEG electron concentration within the quantum well has been a hot issue for decades. Several models have been reported where the electron concentration was calculated analytically as a function of gate-applied voltage[6−10]. However, in the operation time of the HEMT device, the electron concentration changes in two-dimension x and y and depends mainly on the electrical field at the interface. The electrical field at the heterointerface varies from point to point along the channel and is dictated by the nonlinear conductivity in each point along the channel[11−13].

To the authors' knowledge, experimental methods predicting the charge distribution along the channel do not exist yet.

However, several theoretical methods efficiently give a precise prediction of the charge distribution within the active part of the channel, such as the Monte Carlo model[10−14], hydrodynamic model[15,16] (HD), energy balance model (EB), thermodynamic model (TD), and drift-diffusion model (DD)[17, 18].

However, the above-listed models do not account for the quantum properties of 2DEG and rely on the numerical solu-

tions of semiconductor equations self-consistently. The numerical techniques are well known for their computational and time consumption. Moreover, in many cases, the numerical algorithm does not converge very quickly, especially for the HD models. Therefore, analytical models with physically justified approximations will be more efficient for engineering tasks and IC-aimed physics-based models.

Several analytical physics-based models have been developed by different institutions[19−22]. Nevertheless, almost all of the models rely on assumptions posed by the gradual-channel approximation (GCA):

(1) Linear longitudinal electrical field distribution $E(x)$ along the channel. In other words, the electrical field derivative along the channel is constant, thus:

$$\frac{\mathrm{d}E}{\mathrm{d}x} = \text{const.}$$

(2) A constant gradient of the sheet electron concentration $n_s(x)$ along the channel, so:

$$\frac{\mathrm{d}n_s(x)}{\mathrm{d}x} = \frac{n_{\mathrm{di}} - n_{\mathrm{si}}}{L_{\mathrm{ch}}},$$

where n_{di}, n_{si} are the sheet electron concentrations on the drain and source boundaries of the gated region with length L_{ch}.

GCA-based physical models can achieve a good fit with output device performance owing to the fitting process; however, they cannot reveal a deep insight into the device physics, for example, predicting the maximum vertical electrical field $E_\perp \propto q\,[\sigma - n(x)]/\varepsilon$, lattice temperature $T_L \propto E_\parallel J$, and gate current, which is crucially important for the device reliability estimation. The numerical analysis of the RF HEMT struc-

Table 1. Geometrical and simulation parameters of considered GaN/AlGaN HEMT transistor.

| Parameter	Symble	Value	Parameter	Symble	Value
Threshold voltage	V_{off}	−2.1 V	Mobility	μ	2000 cm²/(V·s)
Gate length	L_g	0.1 μm	Saturation velocity	v_s	2.9×10^5 m/s
Gate width	W_g	$4 \times 30\ \mu m$	Exp. parameter	γ_1	2.12×10^{-12}
Barrier thickness	d	30 nm	Exp. parameter	γ_2	3.73×10^{-12}
Channel thikness	W_{ch}	1 μm	Controlling parameters	η_1, η_2	0.5×10^{-2}
Substrate thickness	Ws	100 μm	Controlling parameter	a_1	1
AlGaN dielectric cons	ε	10.66×10^{-11} F/m	Controlling parameter	a_2	5
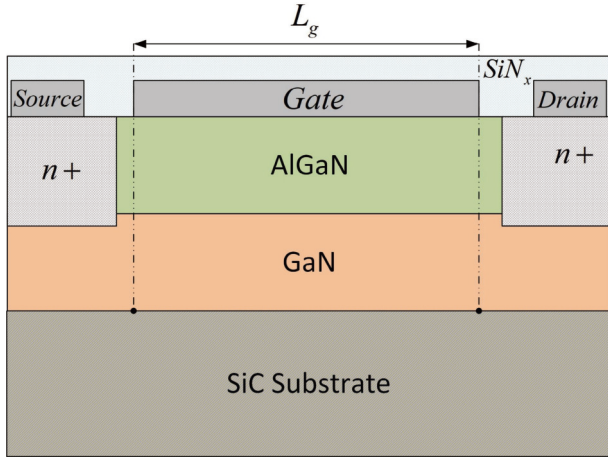
Fig. 1. (Color online) Cross-section of considered GaN/AlGaN HEMT transistor.

ture with a short channel length has proved the GCA to be invalid, as the longitudinal electrical field and electron concentration change in a nonlinear (non-uniform) manner along the channel. Even though the non-uniformity of the electrical field can be found in any position of the channel, the numerical simulations, including the Monte Carlo method[10–14], show that the significant non-uniformity can be found under the gated regions (main gate, a gate connected field plate, a source connected field plate). It is essential to mention that such non-uniformity can be found within the access regions; However, it is relatively less pronounced than in gated regions and mainly happens at relatively high applied voltages. Estimating the electron concentration profile under the gated regions is extremely important as it is related to the electrical field and dissipation power. A robust analytical model for the charge distribution along the channel should be developed to overcome the limitation posed by gradual-channel approximation. This work has been devoted to developing an analytical expression that physically describes the charge variation along the gated part of the channel.

2. Model description

A cross-section of the AlGaN/GaN HEMT transistor discussed in the current research is shown in Fig. 1. Accordingly, the device and simulation parameters are listed in Table 1. The suggested model here is for the active region of the transistor channel under the gate.

Owing to the quantum confinement at the hetero-interface of the HEMT structure, the 2DEG can be described well by Schrodinger's and Poisson's equations[6–8]. Within the triangular quantum well assumption, Schrodinger's and Poisson's

equations can be significantly simplified:

$$n_s(x) = DV_{th} \ln \left\{ \left[e^{\frac{E_f(x)-E_0(x)}{V_{th}}} + 1 \right] \times \left[e^{\frac{E_f(x)-E_1(x)}{V_{th}}} + 1 \right] \right\}, \quad (1)$$

$$n_s(x) = \frac{\varepsilon}{qd}\left(V_g - V_{off} - E_f(x) - V(x)\right), \quad (2)$$

where $E_0(x) = \gamma_0 n_s^{2/3}(x)$ and $E_1(x) = \gamma_1 n_s^{2/3}(x)$ are the two lowest energy levels, D is the density of state, $E_f(x)$ is the Fermi level, V_{th} is the thermal voltage, d and ε are the thickness and dielectric permittivity of the barrier layer, respectively, V_{off} is the cut-off voltage, $V(x)$ is the surface potential along the hetero-interface, V_g is the gate voltage, and γ_0, γ_1 are experimentally defined coefficients.

At the on state, most of the electrons in 2DEG are mainly resided wihin the first quantum energy sub-level $E_0(x)$, which means that the electron concentration portion on the second energy level is comparably smaller. Therefore, their impact on the charge distribution within the channel can be neglected. Considering only the first energy level, Eq. (1) for the sheet electron concentration can be simplified accordingly:

$$\exp\left(\frac{n_s(x)}{DV_{th}}\right) = \exp\left(\frac{E_f(x)-E_0(x)}{V_{th}}\right) + 1. \quad (3)$$

Using Eq. (2) and expression $E_0(x) = \gamma_0 n_s^{2/3}(x)$, along with a series expansion of the left-hand side exponential and rearranging as in Ref. [23], an expression for the surface potential as a function of sheet concentration can be obtained:

$$V_g - V_{off} - V(x) = \frac{qd}{\varepsilon} n_s(x) + \gamma_0 n_s^{2/3}(x) + V_{th} \ln \frac{n_s(x)}{DV_{th}}. \quad (4)$$

Differentiate Eq. (4) with respect to the x, it is easy to determine the electrical field distribution $E(x) = -dV(x)/dx$ along the active part as a function of the sheet concentration and its derivatives:

$$E(x) = -\frac{dV(x)}{dx} = \frac{qd}{\varepsilon}\frac{dn_s(x)}{dx} + \frac{2}{3}\gamma_0 n_s^{-1/3}(x)\frac{dn_s(x)}{dx} + \frac{V_{th}}{n_s(x)}\frac{dn_s(x)}{dx}. \quad (5)$$

It is essential to mention that the electrical field depends not only on the charge distribution but also on the mobility, drift-velocity, temperature and concentration gradients, which can be determined only by solving Poisson and continuity equation self-consistently. Therefore, Eq. (5) should be solved with the current equation self-consistently to determine the charge distribution. As the main target of this work

is to obtain an approximated analytical equation, considering the electron and lattice temperature gradients will make it nearly impossible. Therefore, we assumed the electronic transport is only due to drift diffusive and can be written as,

$$
\begin{aligned}
I_{ds} &= -qW\mu \left[-n_s(x)E(x) - V_{th}\frac{dn_s(x)}{dx} \right] \\
&= -qW\mu \left[n_s(x)\frac{dV(x)}{dx} - V_{th}\frac{dn_s(x)}{dx} \right],
\end{aligned} \tag{6}
$$

where W is the gate width, and μ is the electron mobility. The impact of the temperature gradient will be taken care of through bias-dependent parameters.

Substituting Eq. (5) into Eq. (6) for the drain current, one may obtain the following:

$$
\begin{aligned}
I_{ds} = -qW\mu \Big[n_s(x)\Big(&-\frac{qd}{\varepsilon}\frac{dn_s(x)}{dx} - \frac{2}{3}\gamma_0 n_s^{-1/3}(x)\frac{dn_s(x)}{dx} \\
&- \frac{V_{th}}{n_s}\frac{dn_s(x)}{dx} \Big) - V_{th}\frac{dn_s(x)}{dx} \Big].
\end{aligned} \tag{7}
$$

Rearranging the Eq. (7), one may get:

$$
I_{ds} = -k_0 \frac{d}{dx}\left[k_1 n_s^2(x) + k_2 n_s^{5/3}(x) + k_3 n_s(x) \right], \tag{8}
$$

where $k_1 = qd/2\varepsilon$, $k_2 = 2/5\gamma_0$, and $k_3 = 2V_{th}$ are assumed to be voltage and spatially independent coefficients, and $k_0 = -qW\mu$ is a mobility dependent coefficient (this means it depends on electrical field and temperature as well). The drain current continuity condition states a constant current throughout the device channel, which in turn means that the derivation of current with respect to the x equal to zero. Applying this to Eq. (8), one may have:

$$
\begin{aligned}
\frac{dI_{ds}}{dx} &= \frac{d}{dx}\left(-k_0 \frac{d}{dx}\left[k_1 n_s^2(x) + k_2 n_s^{5/3}(x) + k_3 n_s(x) \right] \right) = 0 \Rightarrow \\
&\frac{d^2}{dx^2}\left[k_1 n_s^2(x) + k_2 n_s^{5/3}(x) + k_3 n_s(x) \right] = 0.
\end{aligned} \tag{9}
$$

In Eq. (9), we neglected the effect of mobility on the electron spatial distribution, and it was taken as averaged value. Eq. (9) is a second-order differential equation that has a solution in the form:

$$
k_1 n_s^2(x) + k_2 n_s^{5/3}(x) + k_3 n_s(x) = C_1 x + C_2. \tag{10}
$$

Eq. (10) is an algebraic high-order equation that is impossible to solve analytically. However, Eq. (10) can be significantly simplified using the underlying physical concept. First of all, Eq. (10) is rearranged as follows:

$$
k_1 n_s^2(x)\left(1 + \frac{k_2}{k_1}n_s^{-1/3}(x) + \frac{k_3}{k_1}n_s^{-1}(x) \right) = C_1 x + C_2. \tag{11}
$$

Let us consider the case where the applied gate voltage is higher than the threshold voltage $V_g > V_{off}$. In such conditions, the first quantified sublevel is much higher than the thermal voltage $E_0(x) = \gamma_0 n^{2/3}(x) \gg V_{th}$. For such a case, the concentration in the channel is high, and the following approximation is valid:

$$
\left(1 + \frac{k_2}{k_1}n_s^{-1/3}(x) + \frac{k_3}{k_1}n_s^{-1}(x) \right) \approx 1, \tag{12}
$$

where $\frac{k_2}{k_1} \approx 10^4$, $\frac{k_3}{k_1} \approx 10^{15}$ and $n_s(x) > 10^{15}$. Correspondingly, Eq. (11) has a solution:

$$
n_s(x) \cong \sqrt{\frac{C_1 x + C_2}{k_1}}. \tag{13}
$$

As the applied voltages approach the threshold voltage, the approximation (12) becomes invalid as:

$$
1 + \frac{k_2}{k_1}n_s^{-1/3}(x) + \frac{k_3}{k_1}n_s^{-1}(x) \gg 1. \tag{14}
$$

Let us consider the case when $\frac{k_2}{k_1}n_s^{-1/3}(x) + \frac{k_3}{k_1}n_s^{-1}(x) \gg 1$. For the electron concentration lower than $n_s(x) < 10^{15}$, the following inequality has a place:

$$
\frac{k_2}{k_1}n_s^{-1/3}(x) \ll \frac{k_3}{k_1}n_s^{-1}(x). \tag{15}
$$

Correspondingly Eq. (11) can be approximated as follows:

$$
k_3 n_s(x) = C_1 x + C_2 \Rightarrow n_s(x) = \frac{C_1 x + C_2}{k_3}. \tag{16}
$$

From Eqs. (13) and (16), the electron concentration distribution along the gated region can be written as follows:

$$
n_s(x) \approx \begin{cases} \sqrt{\dfrac{C_1 x + C_2}{k_1}}, & V_g > V_{off}, \\[2ex] \dfrac{C_1 x + C_2}{k_3}, & V_g \leq V_{off}. \end{cases} \tag{17}
$$

In Eq. (17), C_1 and C_2, are the integration constant, which can be found from the following boundary conditions:

$$
n_s(x = 0) = n_{sL}\left(V_g, V_{off}, E_f(V_L), V_L, T_L \right), \tag{18}
$$

$$
n_s(x = L_g) = n_{sR}\left(V_g, V_{off}, E_f(V_R), V_R, T_L \right), \tag{19}
$$

where V_g is the applied gate voltage, V_{off} is the threshold voltage, $E_f(V_L)$ is the Fermi potential at the left side of the gated region, $E_f(V_R)$ is the Fermi potential at the right side of the gated region, V_L and V_R are the applied intrinsic potential correspondingly at the left and right side of the gated region.

The electron concentration at the boundaries is calculated according to the equations provided in Ref. [6]:

$$
\begin{aligned}
n_s = &\frac{\left(\rho_s + n_i h\exp\left(\dfrac{E_{int} - E_f + \eta_1 V_{eff}}{V_{th}} \right) \right)}{2} \\
&+ \frac{\sqrt{\left(\rho_s + n_i h\exp\left(\dfrac{E_{int} - E_f + \eta_1 V_{eff2}}{V_{th}} \right) \right)^2 + 4(hn_i)^2}}{2},
\end{aligned} \tag{20}
$$

$$
\rho_s = \left(\frac{F}{6} + \frac{2A^2}{3F} - \frac{A}{3} \right)^3, \tag{21}
$$

$$F = \left(108B - 8A^3 + 12\sqrt{-12A^3B + 81B^2}\right)^{1/3},$$
$$A = \zeta\left[(K+1)(\gamma_1 + \gamma_0)\right],$$
$$B = [K + K\delta_1 + \delta_2]V_{th}\xi,$$
$$K = \exp\left(\frac{V_{eff}}{V_{th}}\right), \tag{22}$$

$$\zeta = 1 \bigg/ \left[\frac{1}{DK} + \frac{2(K+1)}{\varepsilon/qd}\right], \tag{23}$$

$$V_{eff} = V_g - V_{off} - V(x), \tag{24}$$

$$V_{eff2} = -\frac{-V_{eff} + \sqrt{V_{eff}^2 + \eta_2}}{2}, \tag{25}$$

where n_s is the 2DEG concentration, D is the density of states of the channel layer, $V_{th} = (kT)/q$ is the thermal voltage, k is the Boltzmann coefficient, T is the channel temperature, q is the elementary charge, $E_f(x)$ is the Fermi potential in Volts, E_i is the ith-quantized energy sublevel in Volts, γ_i is the ith- proportionality coefficient corresponding to E_i, ε is the barrier permittivity, d is the barrier thickness, V_g is the gate potential, V_{off} is the threshold voltage, $V(x)$ is the surface potential, V_{eff} is the effective surface potential, δ_1 and δ_2 are approximation errors, η_1 is a controlling parameter dependence on the potential gradient across the channel, and η_2 is the parameter controlling smooth translation from Fermi statistics to classical Boltzmann statistics. The Eqs. (20)–(25) are straightforward closed-form analytical equations that is continuous with their derivatives , as it was demonstrated in Ref. [6]. The Eqs. (20)–(25) can give an accurate concentration calculation with a maximum error of less than 4% at the threshold compared to the numerical simulation without applying any iteration.

Considering the boundary conditions (18) and (19), the expression for electron concentration distribution (17) can be rewritten as,

$$n_s(x) \cong \begin{cases} \left(\dfrac{\left(n_{sR}^2 - n_{sL}^2\right)x + L_g n_{sL}^2}{L_g}\right)^{\frac{1}{2}}, & V_g > V_{off}, \\[3mm] \dfrac{(n_{sR} - n_{sL})x + L_g n_{sL}}{L_g}, & V_g \leqslant V_{off}. \end{cases} \tag{26}$$

The Eq. (26) gives the charge distribution along the active part of the HEMT transistor for two different operation regimes: above and below the threshold voltage. As one may notice from Eq. (26), the difference between these two regimes is the power of the expressions. At the same time, while deriving Eq. (26), we have neglected the mobility distribution along the channel. To account for non-uniform mobility distribution the Eq. (26) has been unified as follows:

$$n_s(x) \cong \left(\frac{\left(n_{sR}^m - n_{sL}^m\right)x + L_g n_{sL}^m}{L_g}\right)^{\frac{1}{m}}, \tag{27}$$

where $m \approx f(V_g, V_d, \mu, T)$ is the mobility and bias conditions dependent parameter. The function $m(V_g, V_d, \mu, T)$ can be analytically deduced from the continuity equation with the condition $\frac{dI}{dx} = 0$. However, this may complicate the equation, especially when implemented into SPICE program. To simplify the task and find an effective analytical model, we have presented the function $m(V_g, V_d, \mu, T)$ as a function of the applied voltages and extracted the parameters from the numerical simulation:

$$m(V_g, V_d) = a_1\left(V_g - 2V_{off}\right) + a_1\exp\left(-0.7\left(V_d - V_g - V_{off}\right)\right), \tag{28}$$

where a_1, a_2 with the value indicated in Table 1.

It is worth mentioning that the electron concentration n_{sL}, and n_{sR} are functions of the lattice temperature through the thermal voltage as indicated in Eqs. (20)–(25). The channel lattice temperature in our case can be calculated using the physical analytical model presented in Ref. [1].

3. Model verification and discussion

The robust way to examine the model is to compare it with experimentally measured data. Nevertheless, to the author's knowledge, no available experimental method could describe the charge distribution along the channel. The currently existing methodologies, such as capacitance measurement, can only give an average value of charge overall the channel within an interval of uncertainty as well the capacitance measurement can also be conducted while the device is in the off-state. Moreover, besides the intrinsic capacitance, CV measurements include parasitic capacitances, making them a less reliable method of verification. For such reasons, a computational experiment has been carried out.

The simulation object and its physical and geometrical parameters must be the same in both analytical and numerical models to ensure that the comparison takes place. The proposed model considered the only gated region of the GaN HEMT structure as the significant non-uniformity takes place within the gated region; therefore, for the computational experiment, the drain and source ohmic contact was placed directly to the channel without considering the access regions. The channel length, width, barrier, and channel thickness were the same for numerical and analytical models (see Table 1). The semiconductor transport equations within hydrodynamic approximation are the following[16, 17]:

$$j_n = q\mu_n\left(-n\nabla\varphi + \frac{k_B T_n}{q}\nabla n + \frac{k_B n}{q}\nabla T_n\right), \tag{29}$$

$$v_n\nabla v_n = \frac{q}{m_n^*}E - \frac{v_n}{\tau_p}, \tag{30}$$

$$v_n\nabla W_n = -qv_n E - \frac{W_n - W_0}{\tau_m}, \tag{31}$$

$$W_n - W_0 = \frac{3}{2}k_B(T_n - T_L) + \frac{m_n^* v_n^2}{2}, \tag{32}$$

where μ_n is the electron mobility, φ is the electrostatic potential, n is the electron concentration, T_n is the electron temperature, v_n is the drift velocity, m_n^* is the electron effective mass, E is the electrical field, τ_p is the momentum relaxation time, W_n is the electron energy, W_0 is the energy of the transport
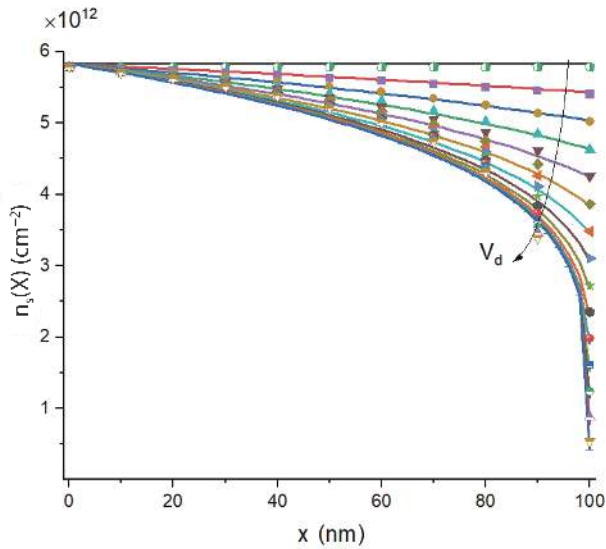
Fig. 2. (Color online) The Electron concentration distribution within the gated region of GaN HEMT at $V_g = 1$ V and swept V_d from 0 to 5 V. In the figure, x denotes the distance along the channel.
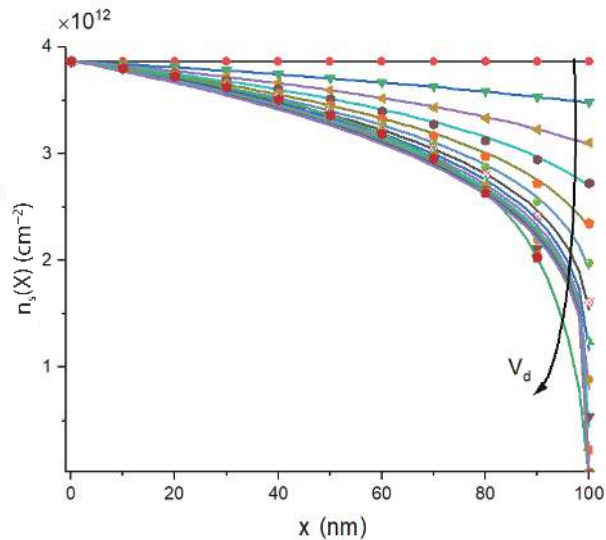

Fig. 4. (Color online) Electron concentration distribution within the gated region of GaN HEMT at $V_g = -1$ V and swept V_d from 0 to 5 V. In figure, x denotes the distance along the channel.

Fig. 3. (Color online) Electron concentration distribution within the gated region of GaN HEMT at $V_g = 0$ V and swept V_d from 0 to 5 V. In the figure, x denotes the distance along the channel.

medium, τ_m is the energy relaxation time, and T_L is the lattice temperature. It is worth noting that electron mobility, momentum, energy relaxation time, and effective mass are related to electron energy, electron temperature, and lattice temperature[24]. The value of parameters for HD simulation was taken from Ref. [24]. The lattice temperature can be determined by the heat equation[24]. The Eqs. (29)–(32), along with the heat equation, were discretized using the semi-implicit scheme to ensure high stability and convergence resulting in a system of nonlinear algebraic equations that has been solved numerically and self-consistently.

Having implemented the hydrodynamic model, we have compared the charge distribution along the channel predicted by the proposed analytical model to the results extracted from the numerical simulation for different bias conditions. Fig. 2 shows the comparison result between the proposed model and numerical hydrodynamic model at gate voltage equal to 1 V and different applied voltage on the drain.
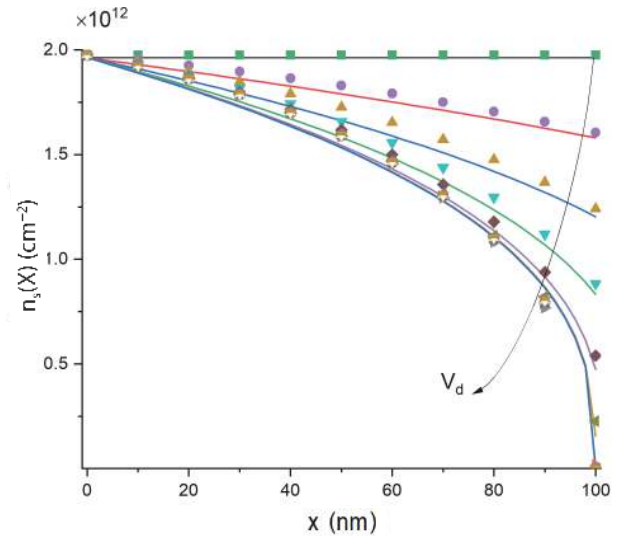
As one may see, the electron concentration is distributed in a non-uniform way, even at small applied voltages. Non-uniform charge distribution leads to non-uniform channel resistivity. Consequently, the potential and electrical field will also have a non-uniform trend. Analysis of non-uniformity of the charge and electrical field distribution is important to gain more information about the device at working conditions as well as to avoid possible reliability issues. The proposed analytical model agrees very well with numerical HD simulation. At applied drain voltage less than saturation voltage, the approximation error did not exceed 2%. The error may increase at relatively high drain voltage spatially in the middle of the active devices due to the mobility averaging and temperature non-uniform distribution.

In the same way, the approximation error at higher drain voltages does not exceed 8%. It is worth mentioning that in the actual device, the upper limit of internal applied drain voltage is determined by the access resistances and the saturation velocity in the drain access resistance. This, in turn, means 8% approximation error will not affect the quality of the analysis as the internal drain voltage does not approach such a high value. A comparison with the HD model reveals that neglecting the quasi-ballistic transport (that may take place in short channel devices) while deriving the analytical equation does not significantly impact the quality of the analysis.

Figs. 3 and 4 demonstrate the electron concentration distribution within the gated region of AlGaN/GaN HEMT for the same applied range of drain voltages and different potentials on the gate. The figures demonstrate a good agreement with numerical simulation. As one may notice, as the gate potential move close to the threshold voltage, the slope of the distribution becomes less than in higher voltage, which the analytical model has predicted well. Such a decrease in slope is explained by the mobility change due to the vertical electrical field along with electron-electron scattering, degree of quantum confinement, and channel temperature. The high agreement between the proposed model and the HD simulation highlights the model's validity and capability to predict

the electron concentration distribution within the gated region of the channel.

4. Conclusion

The research paper presented an analytical expression to predict the charge, electrical field, and potential distributions within the GaN HEMT gated region as a function of applied voltages. The model considers the effect of temperature and mobility on the non-uniformity of the charge distribution. In addition, the model can be used to determine the electric field and potential distributions under the gate, which are highly important for device reliability. The results of analytical modeling highly agree with robust HD numerical simulations; therefore the proposed model can be used as a core equation for a physics-based analytical model that does not rely on the gradual channel approximation.

Acknowledgements

References

[1] Al-Saman A A, Pei Y, Ryndin E A, et al. Accurate temperature estimation for each gate of GaN HEMT with n-gate fingers. IEEE Trans Electron Devices, 2020, 67, 3577

[2] Hoo Teo K, Zhang Y H, Chowdhury N, et al. Emerging GaN technologies for power, RF, digital, and quantum computing applications: Recent advances and prospects. J Appl Phys, 2021, 130, 160902

[3] Meneghini M, De Santi C, Abid I, et al. GaN-based power devices: Physics, reliability, and perspectives. J Appl Phys, 2021, 130, 181101

[4] Zhu G Q, Chang C, Xu Y H, et al. A small-signal model extraction and optimization method for AlGaN/GaN HEMT up to 110 GHz. 2019 IEEE International Conference on Integrated Circuits, Technologies and Applications (ICTA), 2020, 111

[5] Zhu G Q, Chang C, Xu Y H, et al. A millimeter-wave scalable small-signal modeling approach based on FW-EM for AlGaN/GaN HEMT up to 110 GHz. Microw Opt Technol Lett, 2021, 63, 2145

[6] Al-Saman A A, Ryndin E A, Pei Y, et al. An estimation of 2DEG density for GaN HEMT using analytical equation considering the charge conservation low. Solid State Electron, 2022, 188, 108209

[7] Anbuselvan N, Amudhalakshmi P, Mohankumar N. Analytical modeling of 2DEG and 2DHG charge balancing in quaternary $Al_{0.42}In_{0.03}Ga_{0.55}N/Al_{0.3}In_{0.7}NAl_{0.42}In_{0.03}Ga_{0.55}N/Al_{0.3}In_{0.7}N$ HEMTs. J Comput Electron, 2018, 17, 1191

[8] Jena K, Swain R, Lenka T R. Physics-based mathematical model of 2DEG sheet charge density and DC characteristics of AlInN/AlN/GaN MOSHEMT. Int J Numer Model Electron Netw Devices Fields, 2017, 30, e2117

[9] Khandelwal S, Chauhan Y S, Fjeldly T A. Analytical modeling of surface-potential and intrinsic charges in AlGaN/GaN HEMT devices. IEEE Trans Electron Devices, 2012, 59, 2856

[10] Khandelwal S, Goyal N, Fjeldly T A. A physics-based analytical model for 2DEG charge density in AlGaN/GaN HEMT devices. IEEE Trans Electron Devices, 2011, 58, 3622

[11] Ashok A, Vasileska D, Hartin O L, et al. Electrothermal Monte Carlo simulation of GaN HEMTs including electron–electron interac-

tions. IEEE Trans Electron Devices, 2010, 57, 562

[12] Si J, Wei J, Chen W J, et al. Electric field distribution around drain-side gate edge in AlGaN/GaN HEMTs: Analytical approach. IEEE Trans Electron Devices, 2013, 60, 3223

[13] Sadi T, Kelsall R W, Pilgrim N J. Investigation of self-heating effects in submicrometer GaN/AlGaN HEMTs using an electrothermal Monte Carlo method. IEEE Trans Electron Devices, 2006, 53, 2892

[14] Yamakawa S, Goodnick S, Aboud S, et al. Quantum corrected full-band cellular Monte Carlo simulation of AlGaN/GaN HEMTs. J Comput Electron, 2004, 3, 299

[15] Minetto A, Deutschmann B, Modolo N, et al. Hot-electron effects in AlGaN/GaN HEMTs under semi-ON DC stress. IEEE Trans Electron Devices, 2020, 67, 4602

[16] Ryndin E A, Al-Saman A. A novel approach to model high-speed microelectronic switch on the basis of hydrodynamic approximation. International Conference on Micro- and Nano-Electronics 2018, 2019, 128

[17] Wang X D, Hu W D, Chen X S, et al. The study of self-heating and hot-electron effects for AlGaN/GaN double-channel HEMTs. IEEE Trans Electron Devices, 2012, 59, 1393

[18] Asgari A, Kalafi M, Faraone L. A quasi-two-dimensional charge transport model of AlGaN/GaN high electron mobility transistors (HEMTs). Phys E, 2005, 28, 491

[19] Khandelwal S, Chauhan Y S, Fjeldly T A, et al. ASM GaN: Industry standard model for GaN RF and power devices—Part 1: DC, CV, and RF model. IEEE Trans Electron Devices, 2019, 66, 80

[20] Ali Albahrani S, Mahajan D, Hodges J, et al. ASM GaN: Industry standard model for GaN RF and power devices—Part-II: Modeling of charge trapping. IEEE Trans Electron Devices, 2019, 66, 87

[21] Radhakrishna U, Choi P, Grajal J, et al. Study of RF-circuit linearity performance of GaN HEMT technology using the MVSG compact device model. 2016 IEEE International Electron Devices Meeting (IEDM), 2017, 3.7.1

[22] Radhakrishna U, Imada T, Palacios T, et al. MIT virtual source GaN-FET-high voltage (MVSG-HV) model: A physics based compact model for HV-GaN HEMTs. Phys Status Solidi C, 2014, 11, 848

[23] Khandelwal S, Yigletu F M, Iñiguez B, et al. A charge-based capacitance model for AlGaAs/GaAs HEMTs. Solid State Electron, 2013, 82, 38

[24] Palankovski V, Quay R. Analysis and Simulation of Heterostructure Devices. Vienna: Springer Vienna, 2004

Amgad A. Al-Saman was born in Yemen, in 1988. He received the B.Sc. degree (with honours) in electronics and microelectronics and M.S. degree in electronics and nanoelectronics from Southern Federal University, Russia, in 2012 and 2014, respectively. From 2014 to 2018 he was a junior researcher at Scientific and Educational Center "Nanotechnology" at Southern Federal University. At the end of 2018 he was certified researcher. In 2019 he joined the University of Science and Technology of China, Hefei as a Ph.D student. Currently, he is a visiting scholar at Dynax Semiconductor Inc. He has authored multiple international journal and conference publication. His current research interests include physical modelling of semiconductor devices.

Eugeny A. Ryndin was born in Gorlovka, Donetsk region, USSR in 1968. He graduated from the Radiotechnical Institute, Taganrog, Russia in 1992. He received the Ph.D degree in electrical engineering in 1997 and the Doctor of Science degree in 2008. From 1997 to 2004, he was an Associate Professor with the Electronic Apparatuses Design Department, Taganrog State University of Radioengineering. From 2004 to 2008, he was a Senior Researcher with the Southern Scientific Center, Russian Academy of Science, Rostov-on-Don. From 2008 to 2019, he was a Professor with the Institute of Nanotechnologies, Electronics and Electronic Equipment Engineering, Southern Federal University, Taganrog. Since 2019, he has been a Professor with the Micro- and Nanoelectronics Department, Saint Petersburg Electrotechnical University "LETI", Saint Petersburg. His research interests include micro- and nanoelectronic elements development and numerical modeling, MEMS development and VLSI design.

Fujiang Lin received the B.S. and M.S. degrees from the University of Science and Technology of China (USTC), Hefei, China, in 1982 and 1984, respectively, and the Dr.-Ing. degree from the University of Kassel, Germany, in 1993, all in electrical engineering. His research interest is in the development of CMOS as a cost-effective technology platform for 60-GHz band millimeter-wave SoC, as well as millimeter wave therapy for healthcare applications. He is initiator and co-organizer of international workshops and short courses at APMC99, SPIE00, ISAP06, and IMS07. Dr. Lin was the recipient of the 1998 Innovator Award presented by EDN Asia Magazine. He has authored or coauthored over 150 scientific papers. He holds over 50 patents.

Yi Pei received the B.S degree in Electrical Engineering from Peking University, Beijing, China, in 2004, the M.S and Ph.D degrees in Electrical Engineering from University of Santa Barbara, U.S.A, in 2005 and 2009, respectively. He is currently the V.P. of technology, in charge of GaN product design, cutting edge GaN technology development and I.P. strategy. His research interests include microwave and millimeter wave GaN electronics design and modeling, GaN power electronics design and application, and Ⅲ-N semiconductor processing technology development. He is the author or coauthor of more than 100 journal and conference papers. He also holds more than 150 granted patents and patent applications.